Consiglio Nazionale delle Ricerche

On the Estimates of the Ring Current Injection and Decay

P. Ballatore, W.D. Gonzalez

2002-TR-22

On the Estimates of the Ring Current Injection and Decay

P. Ballatore

ISTI/CNR, via Moruzzi, 1 - 56124 Pisa - Italy

W. D. Gonzalez

National Institute for Space Research (INPE), Sáo José dos Campos - Brazil

Abstract. In the context of the space weather predictions, the forecast of the ring current strength (and of the *Dst* index) based on the solar wind upstream conditions is of specific interest for predicting the occurrence of geomagnetic storms. At the same time, it is of interest to study separately its two components: (1) the injection from the interplanetary space and (2) the *Dst* decay. In the present paper, we have verified the validity of the Burton's equation for estimating the ring current energy balance using the equatorial electric merging field instead of the original VB_S parameter. Then, based on this equation, we have used the phase space method in order to determine the best-fit approximations for the ring current injection and decay as functions of the equatorial merging electric field. Results indicate that the interplanetary injection is statistically higher than in previous estimations using VB_S, while the decay is faster. The effects of these two components are compensated, so that the statistical *Dst* predictions using the equatorial electric merging field or using VB_S are about equivalent.

Categories and Subject descriptors: *(ACM) – G.3 Probability and statistics, I.6 Simulation and modeling, J.2 Physical science and engineerin; (PACS) – 94.30.-d Physics of the magnetosphere, 94.30.Jp Ring currents.*

1. Introduction

The possibility of forecasting the geomagnetic activity and the occurrence of geomagnetic storms can be considered as one of the main goals in recent space science investigations. The most commonly used index of geomagnetic storms is the *Dst* index, so that the possible *Dst* predictions have been widely studied and accurate estimates of *Dst* can be presently computed based on interplanetary space observations [O'Brien and McPherron, 2000a].

The *Dst* index is derived from the perturbations of the horizontal component of the geomagnetic field as measured by mid-latitude (or latitudes at about 20°- 30° from the CGM, Corrected GeoMagnetic, equator) ground stations and it is expressed in nT units. It represents the westward ring current formed around the Earth and associated with the occurrence of the geomagnetic storms [Mayaud, 1980; Gonzalez et al., 1994]. In particular, the energy balance of the ring current is carried by energetic ions injected into the magnetosphere mostly by the mechanisms of reconnection between the interplanetary magnetic field (IMF) and the magnetospheric field. Generally, reconnection occurs when the two fields have opposite directions, and, at the sub-solar point, this is so when the IMF is directed southward (in the GSM coordinate system). Therefore the ring current energy input is considered proportional to the upstream parameter VB_s, where V is the solar wind speed and B_s is the southward IMF B_z component [Burton et al., 1975]. In fact the original ring current energy balance equation is:

$$\Delta Dst^*/\Delta t = Q - Dst^*/\tau \qquad [1]$$

Where τ is a constant rate of decay of *Dst* and Q is the ring current energy injection expressed as a linear function of VB_s [Burton et al., 1975]. In eq. 1, Dst^* indicates a *Dst* corrected after the effect of the solar wind pressure (or the associated magnetospheric currents):

$$Dst^* = Dst - b \cdot P^{1/2} + c \qquad [2]$$

where P is the solar wind pressure, b and c are constants.

A review paper by O'Brien and McPherron [2000a] summaries and compares the previous *Dst* forecasts. The models considered are all corresponding to the differential Eq. 1, which was originally reported by Burton et al. [1975]. Each model differs from

the others for the different values or functions derived for the Q and τ and for the values of the constants b and c involved in the expression of the pressure correction (Eq. 2). Compared with other models, a more elaborated one was derived by O'Brien and McPherron [2000b], who considered Q and τ as functions of VB_s and derived b and c (in Equation 2) equal to 7.26 nT/nPa$^{1/2}$ and 11 nT, respectively. The Q function is different from zero only during southward IMF and, at this time, it is:

$$Q\ [nT/h] = -4.4(VB_S\ [mV/m] - 0.49) \qquad [3]$$

The decay rate, τ, is a function of VB_s and it is:

$$\tau[h] = 2.4e^{9.74/(4.69+VB_S[mV/m])} \qquad [4]$$

The equations 3 and 4 represent the most efficient functions giving *Dst* forecasts according to equations 1 and 2. Therefore the related Q and τ can be considered, respectively, as the *effective* ring current interplanetary energy injection and decay. Although these considerations, it might be questioned how much these *effective* Q and τ differ from the real ones. In fact it is known that other quantities represent the interplanetary - magnetospheric reconnection differently of the VB_S parameter. In particular, the equatorial projection of the merging electric field (E_m) is very similar to VB_S, in fact it represents the rectified reconnection electric field in the equatorial plane. Specifically, the equatorial E_m is taking into account effects due to the IMF B_y component and the IMF clock angle so that contributions from the reconnections at the magnetospheric lobes are included. Specifically E_m coincides with VB_S in the case of clock angle close to ±180 or IMF $B_y << B_z$ with negative B_z.

The equatorial electric field that we consider in the following is [Kan and Lee, 1979; Akasofu, 1981]:

$$E_m = V \cdot B_t \cdot \sin^2(\phi/2) \qquad [5]$$

Where B_t is the projection of the IMF on the Y-Z plane (in GSM coordinate system) and ϕ is the clock angle between B_t and the Z-axis [Kan and Lee, 1979]. In the following, we indicate as 'E_m' the equatorial electric merging field given in Eq. 5, which is different of the global electric merging field [Gonzalez, 1990] and closer to the level of the previously used VB_S parameter.

This paper deals with the best-fit approximations for the ring current injection and decay as functions of E_m. Conclusions are based on the comparison between the present results and previous findings using VB_S instead of E_m.

2. Data analysis and observations

The time interval under investigation is the period since January 1st, 1995 until December 31st, 2000. For this period, the interplanetary data considered are the measurements of IMF components and V from the OMNI/NSSDC database. According to data availability, these measurements are from different satellites, mostly from WIND, but smaller amounts of data are from IMP-8 and ACE. These measurements have been used to calculate the VB_s and E_m parameters.

A delay is introduced between the ground based *Dst* index and the interplanetary data. This delay is chosen equal to 1-h in agreement with previous estimations of average delays between satellites and ground-based measurements [e.g., Ballatore et al., 2001]. It is worth mentioning that the 1-h delay is valid on statistics bases but not exactly at any specific time.

If equation 1 is valid, we can calculate the offset and the slope of the linear best-fit for the scatter plots representing ΔDst vs. *Dst* and we can derive Q and τ from the following equation

$$offset = Q\,\Delta t \qquad [6]$$

$$slope = -\Delta t/\tau \qquad [7]$$

Considering all the data together the determination of the offset and slope of the best-fit are not statistically significant due to the large scatter of data. This is in agreement with the important dependence of Q and τ on the interplanetary parameters [e.g., Fenrich and Luhmann, 1998]. However, if each scatter plot is limited only to data points with restricted intervals of VB_S, the obtained best-fits are significant, and Q and τ determination (from eq. 6 and eq. 7) can be considered statistically significant too [O'Brien and McPherron, 2000a].

We have calculated the best-fits for the scatter plots ΔDst vs. Dst considering separately data corresponding to separate 1 mV/m intervals of E_m, starting from 0.05 mV/m until 12.5 mV/m. The linear correlations for each best-fit are significant at a confidence level above 99.9% until E_m ~ 10.5 mV/m, but the best precision is related to intervals with E_m < 8 mV/m, where most of the interplanetary occurrence is observed. Above ~ 10.5 mV/m, the confidence level for the best fits are < 99.0%, due to the small number of data points involved. In any case, the Q and τ derived from eq.s 6 and 7 are reported in Figure 1 and 2 as a function of the corresponding E_m (the data points are shown at the center of the 1 mV/m E_m interval to which they refer).

We have studied linear and non-linear fits in Figures 1 and 2 between Q vs. E_m and τ vs. E_m, respectively. The best-fits chosen for $Q(E_m)$ and $\tau(E_m)$ (reported on the plots) are the ones corresponding to the best correlation coefficients and the smallest residuals. The possibility of defining statistically significant best fits can be interpreted as the validity of Burton's equation (Eq. 1) by using E_m instead of VB_S.

2.1. Ring current injection Q

While the best fit between VB_s and Q is linear [O'Brien and McPherron, 2000b], the best fit between E_m and Q is found to be a double logarithmic function. This may suggest a more direct relationship between the sub-solar point reconnection and the ring current energy input and a higher effect of the magnetospheric/ionospheric re-processing on reconnection occurring at the lobes.

Previously, a similarly non-linear relationship was found by Akasofu [1981], between the energy coupling ε [$\varepsilon = V \cdot B^2 \cdot L^2 \cdot \sin^4(\phi/2)$, where B is the module of the total IMF vector and L is a scale length at the magnetopause] and the Dst index. In this case, the best-fit was as a second order polynomial function in $\log(\varepsilon)$. This was explained by considering that a more intense ring current forms closer to the Earth, namely in the atmosphere of an exponentially increasing density.

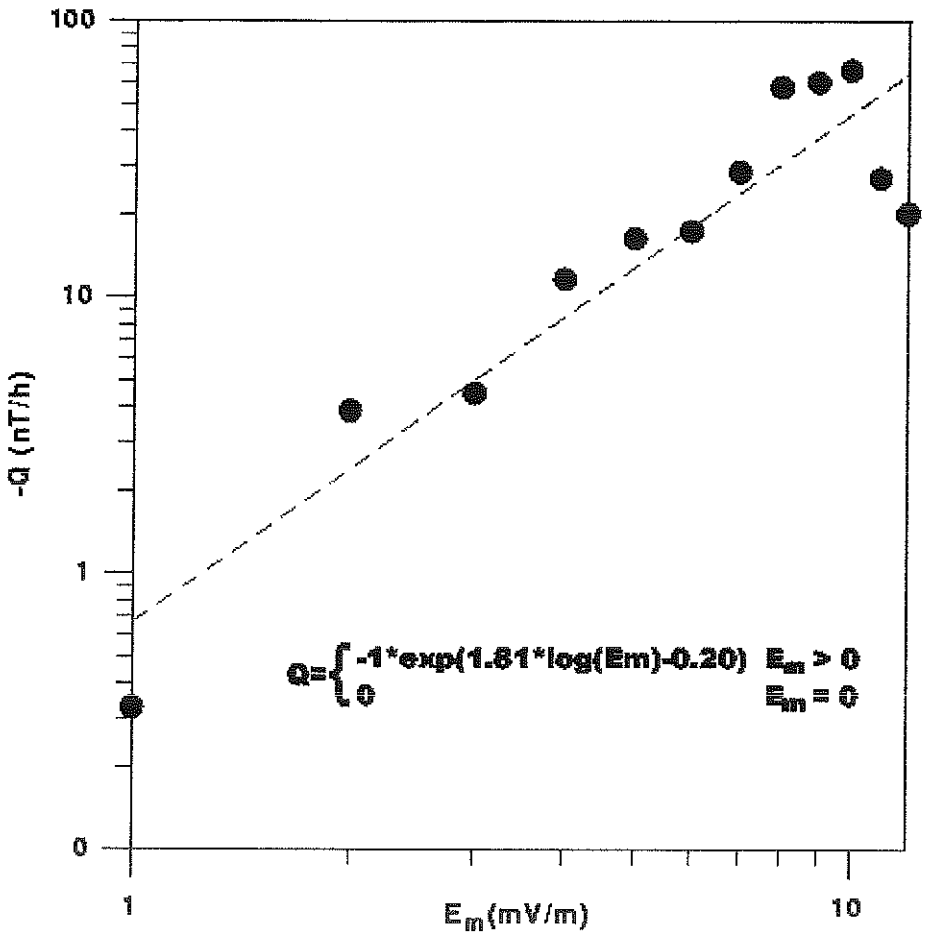

Figure 1. *Injection Q versus E_m. Q values are derived from linear fits to the phase space ΔDst vs. Dst for separate 1mV/m Q intervals; each point is shown at the center of the E_m interval to which it refers.*

In order to estimate quantitatively the value of the injection Q derived from the best-fit reported in Figure 1, we have studied the comparison between the function $Q(VB_s)$ calculated according to O'Brien and McPherron [2000b] and the $Q(E_m)$ function given by:

$$log(-Q(E_m)\ [nT/h]) = 1.81 \cdot log(E_m[mV/m])-0.2 \qquad [8]$$

In Figure 3, the number of occurrences of $Q(E_m)$ and $Q(VB_s)$ are reported for separate ranges of the IMF clock angle during negative IMF B_z (three top panels), and during northward IMF (bottom panel).

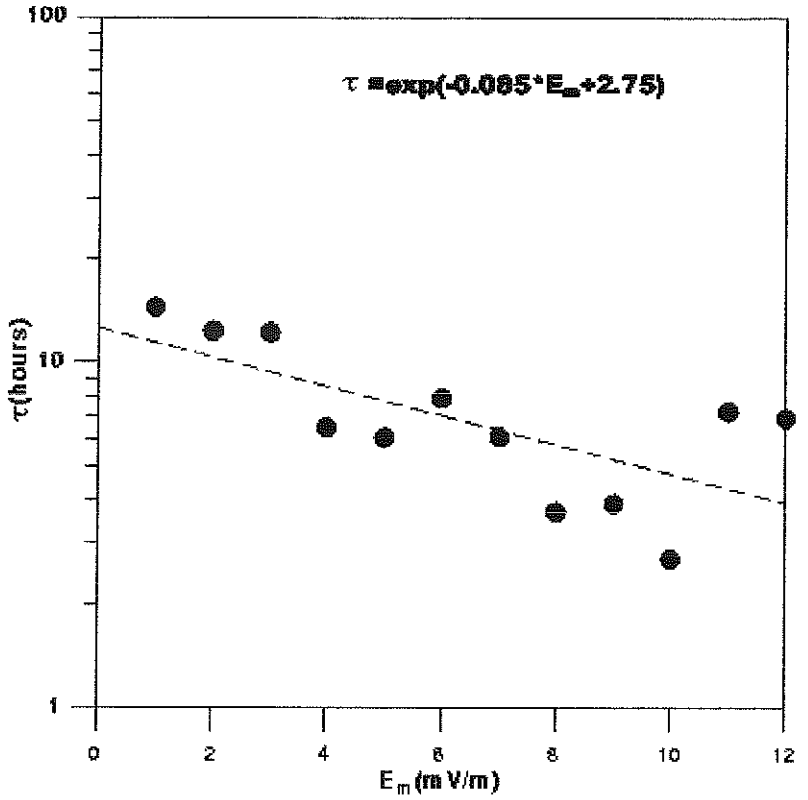

Figure 2. *Decay τ versus E_m. τ values are derived from linear fits to the phase space ΔDst vs. Dst for separate 1mV/m Q intervals; each point is shown at the center of the E_m interval to which it refers.*

In Figure 3, each point is illustrated at the center of the 5 nT/h Q interval to which it refers. It can be seen that the distribution of $Q(VB_s)$ is clustered at zero, with maximum total occurrence (the total occurrence is the sum of the occurrence in the three upper panels of Figure 3) in the range between -5 and 0 nT/h. Differently, the distribution of $Q(E_m)$ is shifted towards higher injection values, with maximum occurrence in the range between −10 and -5 nT/h in each one of the three upper panels in Figure 3. The shift between $Q(Em)$ and $Q(VB_S)$ is especially clear for IMF clock angle $|\phi|$ closer to 90°, when the number of occurrences of $Q(E_m)$ is always higher than $Q(VB_s)$ for intervals of $Q < -5$ nT/h.

The bottom panel of Figure 3 shows the distribution of data points with $Q(E_m)$ different of zero for periods with northward IMF, when $Q(VB_s)$ is always equal to zero.

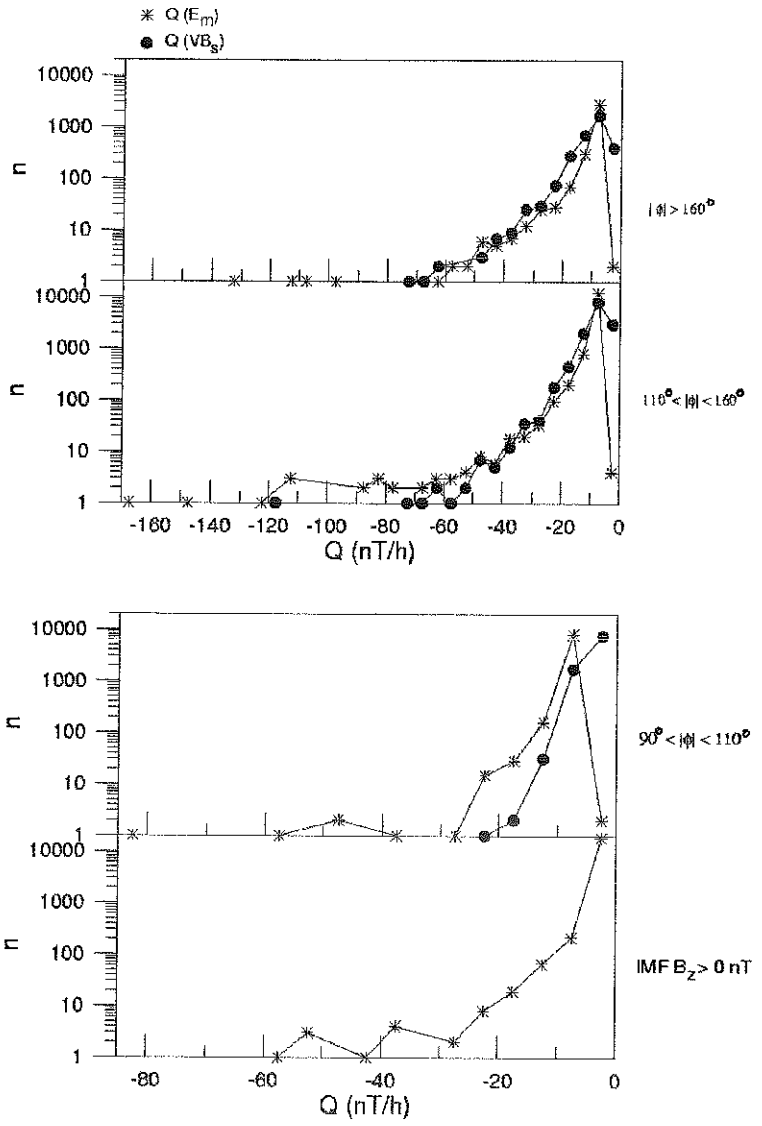

Figure 3. *Number of Q occurrences in the 5 nT/h intervals whose center is indicated on the abscissa. Each panel refers to periods when the clock angle was in the range indicated on the right. The bottom panel refers to periods of IMF $B_z > 0$.*

Although, in this panel, most of the $Q(E_m)$ occurrences are clustered towards zero, a significant percentage of data lies in the range (-25, 0) nT/h.

2.2. Ring current decay τ

The ring current decay τ calculated by O'Brien and McPherron [2000a] was based on the hypothesis that an increase in VB_s (i.e., during a higher magnetospheric convection electric field) is associated with a shift towards lower altitudes of the boundary between open and closed drift orbits. At lower altitudes the denser exosphere provides a more rapid charge exchange interactions, resulting in a more rapid decay of the ring current [O'Brien and McPherron, 2000b]. In particular, it is assumed that τ is related to the charge exchange lifetime, $\tau \propto n_H^{-1}$, where n_H is the density of hydrogen in the geocorona [Smith and Bewtra, 1978]. In addition, the geocorona density falls with distance from the Earth, L, as $n_H \propto e^{-L/L_0}$, where L_0 is a scale height determined by atmospheric and gravitational parameters [Smith and Bewtra, 1978]. Therefore, O'Brien and McPherron [2000b] considered

$$\tau \propto e^{L/L_0} \qquad [9]$$

where L is the distance from the Earth and L_0 is the scale height mentioned above. Considering Φ_0 as the electric field strength proportional to the polar cap potential drop, O'Brien and McPherrom [2000b] approximated

$$L^{-1} \propto \Phi_0 \qquad [10]$$

Further, they included the result obtained by Reiff et al. [1981]

$$\Phi_0 \propto (a' + VB_s) \qquad [11]$$

Finally, O'Brien and McPherron [2000b] derived

$$\tau(VB_s)\,[h] \propto e^{(a' + VB_s)^{-1}} \qquad [12]$$

Roughly, Eq. 2 indicates that a decrease in $\tau(VB_s)$ is associated to an increase in VB_s. Similarly, in our case, we find that a decrease in $\tau(E_m)$ is associated to an increase in E_m, with the best functional form given by (see Figure 2)

$$\log(\tau(VB_s)\,[h]) = -0.085 \cdot E_m[mV/m] + 2.75 \qquad [13]$$

The comparison between $\tau(E_m)$ and $\tau(VB_S)$ shows that, for equivalent E_m and VB_S, $\tau(VB_S)$ is generally larger than $\tau(E_m)$, indicating a faster *Dst* decay associated to $\tau(E_m)$. In fact, for E_m or VB_S in the range (0, 12) mV/m, $\tau(E_m)$ varies in the interval (14.88, 2.9) h while $\tau(VB_S)$ varies in the interval (17,73, 4.29) h.

2.3. Pressure correction

The correction to *Dst*, introduced in Eq. 2 and related to the solar wind pressure P, takes into account the contribution to the ring current energy balance due to magnetospheric currents [e.g., Burton et al., 1975; O'Brien and McPherron, 2000b]. In order to estimate this pressure correction, we use the following procedure (similar to O'Brien and McPherron, 2000b): for separate intervals of pressure variations, the differences between the phase space best-fit offsets and Q(Em) (given in Eq. 8) are calculated for separate E_m intervals. In each pressure variation range, this is done for each E_m interval in which there is a relatively sufficient number of data points. In this case the definition of the offset given in Eq. 6 is extended to

$$offset - Q\Delta t = b \cdot sqrt(P)|_{Q,Dst} \qquad [14]$$

More specifically, 1-h data points for the whole period 1995-2000 have been grouped for separate 0.2 $nPa^{1/2}$/h intervals of variation $\Delta P^{1/2}$. Then, separately for each of these groups, a procedure similar to that used for deriving Figure 1 has been repeated to find the offsets for separate intervals of E_m. Finally, the differences between these offsets (in units nT/h) and $Q(E_m)$ calculated from Eq. 8 have been found. We report these differences in Figure 4 with respect to the center of the corresponding 0.2 $nPa^{1/2}$/h interval of $\Delta P^{1/2}$.

From eq. 14 and the best-fit obtained in Figure 4, we derive the coefficient b (that is the same b given in Eq. 2 and Eq. 14) as ~4.68. To calculate the pressure correction's parameter c (given in Eq. 2), we make use of the Eq.s 14 and 15 given by O'Brien and McPherron [2000b] and our results given in Figure 4. In this way, we obtain a value of c equal to 7.25 nT. This value is smaller than the value 11 nT calculated for VB_s [O'Brien and McPherron, 2000b]. In addition, this is also smaller than the original value of 20 nT, derived by Burton et al. [1975].

2.4 Comparisons among *Dst* and its estimates as functions of VB_s and E_m

The *Dst* forecast has been computed using interplanetary parameters according to Eq. 1 and the functions $Q(VB_s)$ and $\tau(VB_s)$ given in Eq. 3 and 4. In this way the $Dst(VB_s)$ is calculated as reported by O'Brien and McPherron [2000a; 2000b]. Similarly, the

$Dst(E_m)$ has been derived by using the Eq. 1 with $Q(E_m)$ and $\tau(E_m)$ functions given in Eq. 8 and 13, respectively.

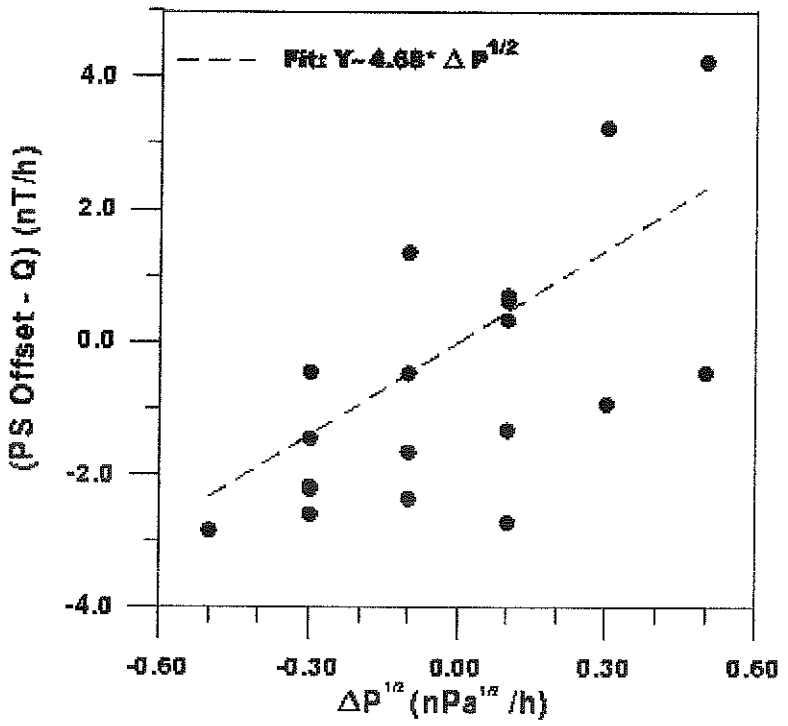

Figure 4. *Residual of phase space offsets minus the injection Q versus variations of the solar wind dynamic pressure P. The equation reported corresponds to the best fit and the coefficient 4.68 is the constant b in Eq. 2.*

As a further verification of the validity of Eq. 1 for the use of E_m and also to estimate the possible precision of the *Dst* forecast obtained by E_m, we studied the comparisons between $Dst(E_m)$, $Dst(VB_s)$ and the observed *Dst* index. In Figure 5 the distributions of the differences $Dst\text{-}Dst(E_m)$ and $Dst\text{-}Dst(VB_s)$ are reported for separate ranges of the IMF clock angle. Both distributions maximize in the range (-5, 5) nT, where a percentage of data points > 70% is observed. This indicates the good precision of both $Dst(VB_s)$ and $Dst(E_m)$ predictions. In addition, the percentage of occurrences in the range (-5, 5) nT for $Dst(E_m)$ is about the same as the distribution $Dst(VB_s)$. Therefore, the prediction of the ring current level made by E_m can be considered as significant as that made by VB_s. In particular, in Figure 5, the distributions related to $Dst(E_m)$ and $Dst(VB_s)$

are very much similar for the clock angle ϕ in the range (-70, 70)°, namely, during the most northward IMF values.

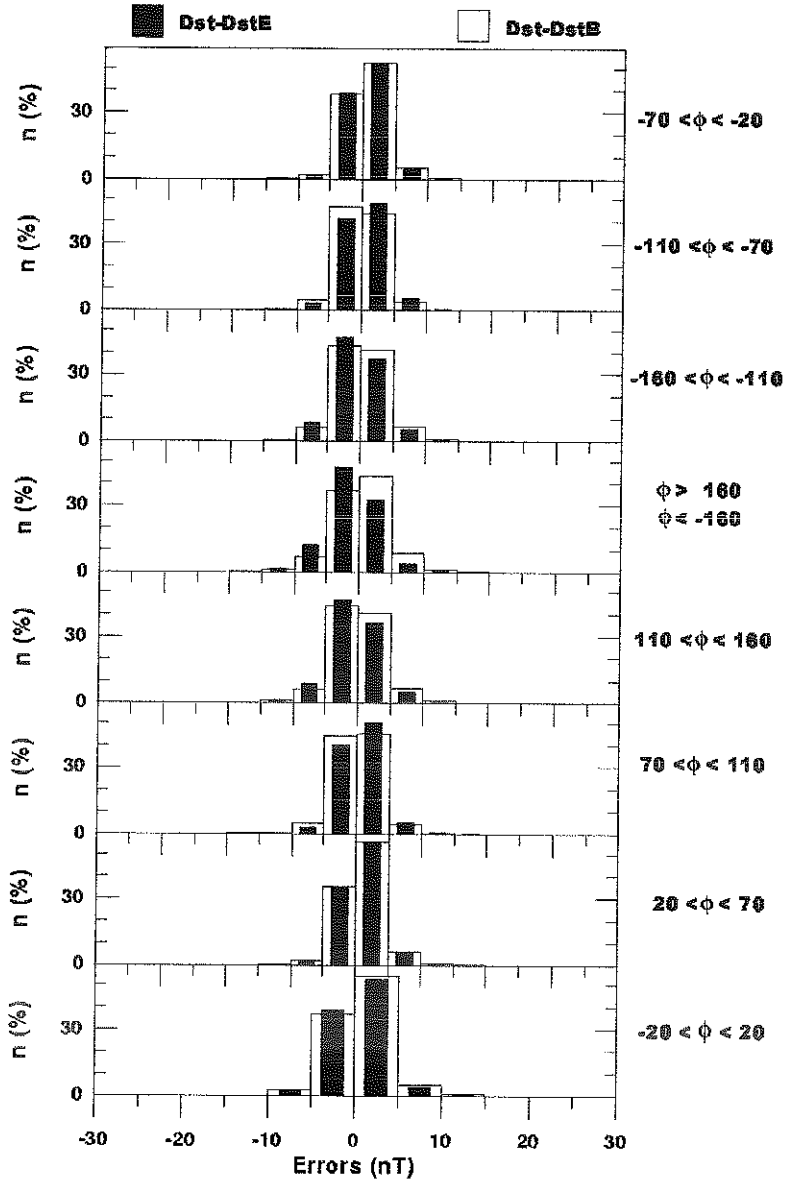

Figure 5. *Distributions of the differences Dst-Dst(E_m) and Dst-Dst(VB_s). Each panel refers to periods when the clock angle lies as indicated at the right of the plot.*

We note that, in Figure 5, the occurrence of differences in the positive range of the abscissa are corresponding to the occurrence of a *Dst* less disturbed than $Dst(E_m)$ or $Dst(VB_s)$, i.e. $Dst(E_m)$ or $Dst(VB_s)$ over-estimates the experimental *Dst*. Similarly, the occurrence of differences in the negative range of the abscissa indicates that the corresponding $Dst(E_m)$ or $Dst(VB_s)$ under-estimates the experimental *Dst*, which is more disturbed. Therefore, Figure 5 shows that, for ϕ around $\pm$ 90°, $Dst(E_m)$ tends to over-estimate the observed *Dst*, while this is not so for $Dst(VB_s)$. In fact, for ϕ in the interval (70, 110)° & (-110, -70)°, the occurrence of $Dst-Dst(E_m)$ is higher in the positive range of differences, while the occurrence for $Dst-Dst(VB_s)$ in the positive range is equal to or higher than in the negative range. On the other hand, for the most southward oriented IMF values (ϕ around $\pm$ 180°), $Dst(E_m)$ tends to under-estimate the *Dst* index, while $Dst(VB_s)$ tends to over-estimate it. These observations are in agreement with the occurrence of higher merging observed in Figure 3 for clock angles closer to |90°|.

Figures 5 and 6 show that the observed results are rather symmetrical for positive or negative clock angle ranges, so that no significant differences are presently obtained for positive or negative IMF B_y periods considered separately.

A more direct comparison between $Dst(E_m)$ and $Dst(VB_s)$ is given in Figure 6, where the distributions of the differences $Dst(E_m)-Dst(VB_s)$ are reported for separate ranges of the IMF clock angle. It is shown that $Dst(VB_s)$ tends to indicate a ring current activity higher than $Dst(E_m)$ does, except at clock angles around $\pm$ 90° (ϕ=(-110, -70) and ϕ=(70, 110), when $Dst(E_m)$ is more disturbed. The higher ring current level indicated by $Dst(VB_s)$ is not due to the higher injection $Q(VB_s)$, which is null always during northward IMF and tends to be smaller than $Q(E_m)$ also during the other periods (as indicated in Figure 3). Therefore the higher disturbance indicated by $Dst(VB_s)$, compared with $Dst(E_m)$, is evidently related to the fact that $\tau(VB_s)$ is higher than $\tau(E_m)$, as specified in the previous paragraph 2.2. The slower decay of the ring current given by $\tau(VB_s)$ seems well compensating the absence of injection considered during northward IMF. At the same time, the real value of the ring current decay should be closer to $\tau(E_m)$, as it can be deduced considering that the real interplanetary-magnetospheric merging has to include also inputs from magnetospheric-lobe effects, as in the expression of the equatorial electric merging field E_m [Kan and Lee, 1979; Akasofu, 1981] and differently of VB_S.

Further studies considering the effects of total electric merging field on the ring current injection and decay are in course of development.

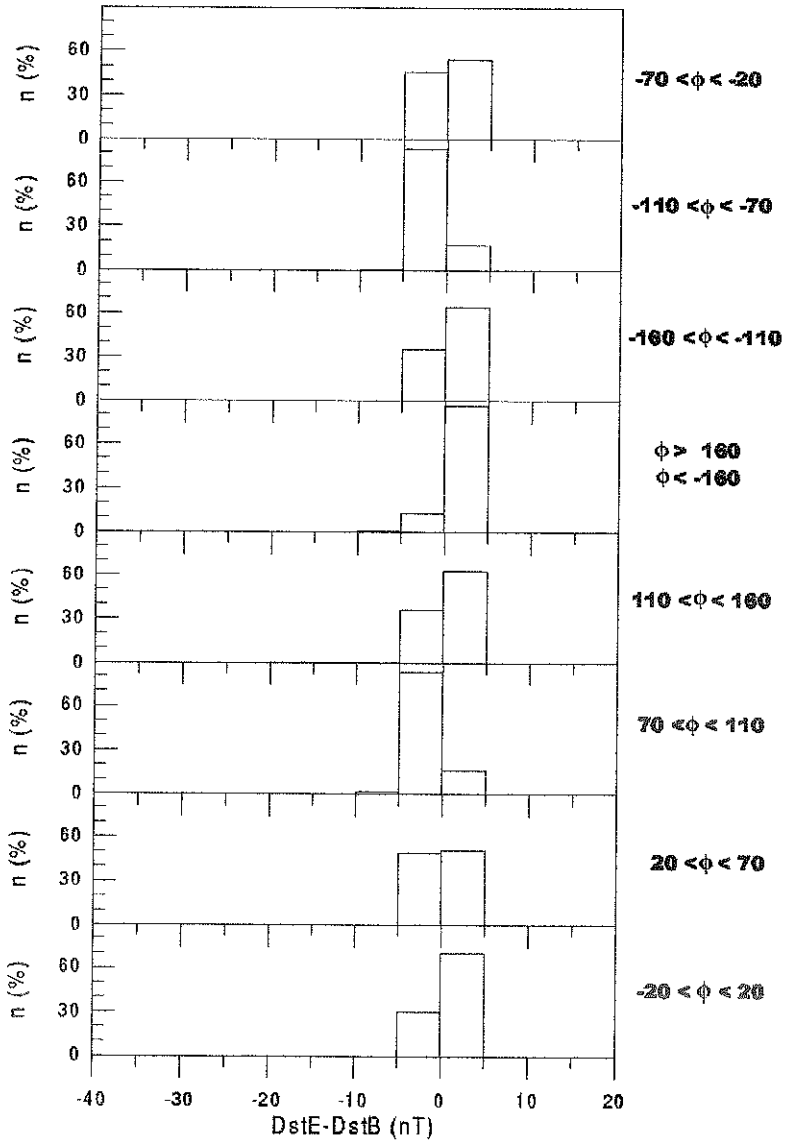

Figure 6. *Distribution of the differences $Dst(E_m)$-$Dst(VB_s)$. Each panel refers to periods when the clock angle lies as indicated at the right of each plot.*

3. Conclusions

The present study of the ring current energy balance demonstrates the validity of the Eq. 1 [Burton et al., 1975] for the use of E_m instead of the parameter VB_s. In fact, the *Dst* predictions obtained using E_m in this equation correspond to the observed *Dst* as well as previous *Dst* forecasts. In particular, the use of E_m and of Eq. 1 in *Dst* predictions gives new functional forms for the ring current injection (Q) and decay (τ).

The estimate of Q as a function of E_m indicates the occurrence of an interplanetary injection greater than that calculated using VB_s. This effect is particularly evident for IMF clock angles $|\phi|$ closer to 90°, when the reconnection between the magnetosphere and the interplanetary magnetic field is more active on the magnetospheric lobes. In addition, during positive IMF B_z periods, when Q calculated using VB_s is always zero [Burton et al., 1975; O'Brien and McPherron, 2000a, 2000b], the injection estimated using E_m is generally in the range (0, 25] nT.

The prediction of the rate of ring current decay, τ, obtained by using E_m indicates that the real loss should be more rapid than that calculated in previous forecasts.

Acknowledgments. The interplanetary data and the geomagnetic index *Dst* are from the OMNI database, U.S. National Space Science Data Center (NASA, Goddard Space Flight Center, USA).

References

Akasofu, S.-I., Energy coupling between the solar wind and the magnetosphere, *Space Sci. Rev.*, 28, 121, 1981.

Ballatore, P., J.P. Villain, N. Vilmer, and M. Pick, The influence of interplanetary medium on SuperDARN scattering occurrence, *Ann. Geophysicae*, 18, 1576, 2001.

Burton, R.K., R.L. McPherron, and C.T. Russell, An empirical relationship between interplanetary conditions and *Dst*, *Journ. Geophys. Res.*, 80, 4204, 1975.

Fenrich, F.R., and J.G. Luhmann, Geomagnetic response to magnetic clouds of different polarity, *Geophys. Res. Lett.*, 25, 2999, 1998.

Gonzalez, W.D., A unified view of solar wind-magnetosphere coupling functions, Planet. Space Sci., 38, 627, 1990.

Gonzalez, W.D., J.A. Joselyn, Y. Kamide, H.W. Kroehl, G. Rostoker, B.T. Tsurutani, and V.M. Vasyliunas, What is a geomagnetic storm ?, *Journ. Geophys. Res.*, 99, 5771, 1994.

Kan, J.R., and L.C. Lee, Energy coupling function and solar wind-magnetosphere dynamo, *Geophys. Res. Lett.*, 6, 577, 1979.

Mayaud, P.N., Derivation, meaning and use of geomagnetic indices, *Geophys. Monograph*, vol. 22, AGU, Washington, DC, 1980.

O'Brien, T.P., and R.L. McPherron, Forecasting the ring current index *Dst* in real time, *J.A.S.T.P.*, 62, 1295, 2000a.

O'Brien, T.P., and R.L. McPherron, An empirical phase space analysis of ring current dynamics: Solar wind control of injection and decay, *Journ. Geophys. Res.*, 105, 7707, 2000b.

Reiff, P.H., R.W. Spiro, and T.W. Hill, Dependence of polar cap potential drop on interplanetary parameters, *Journ. Geophys. Res.*, 86, 7639, 1981.

Smith, P.H., and N.K. Bewtra, Charge exchange lifetime for ring current ions, *Space Sci. Rev.*, 22, 310, 1978.